

Outdoor performance evaluation of a novel photovoltaic heat sinks to enhance power conversion efficiency and temperature uniformity

E.Z. Ahmad^{a,b}, K. Sopian^a, A. Fazlizan^a, H. Jarimi^a, A. Ibrahim^{a,*}

^a Solar Energy Research Institute, Universiti Kebangsaan Malaysia, 43600, Bangi, Selangor, Malaysia

^b Faculty of Electrical & Electronic Engineering Technology, Hang Tuah Jaya, 76100, Durian Tunggal, Melaka, Malaysia

ARTICLE INFO

Keywords:

Passive heat sink
PV module Temperature
Power conversion efficiency
Temperature uniformity

ABSTRACT

The non-uniformity of photovoltaic (PV) temperature can further deteriorate its power conversion efficiency and technical lifetime over long field exposures. This study proposed novel fins for a PV module temperature reduction and enhancing temperature uniformity. The proposed multi-level fin heat sinks (MLFHS) consist of a novel geometry of extruded aluminum material attached to the rear side of the PV module. The developed outdoor experimental setup consists of two identical 120 Wp monocrystalline PV modules; one served as a reference module for comparison against the module with the proposed novel heat sink geometry. The temperature distributions across PV modules and the electrical parameters were then recorded and analysed. A substantial drop in the module temperature of 8.45 °C was observed at solar irradiance and ambient temperature of 941 W/m² and 36.17 °C, respectively. As a result, the heat sink improved the overall power output up to 9.56% under outdoor operating conditions. Furthermore, the prominent effect of temperature uniformity was perceived for solar irradiance greater than 600 W/m² and improved by 14.8%. These findings are foundational for passive cooling methodologies to guide further research and development of an efficient PV cooling methodology.

1. Introduction

Renewable energy is regarded as the second most significant contributor to electricity generation after coal. Despite the lower percentage than conventional technologies in the energy mix, a very steep progression can be observed in the electricity generation from photovoltaic (PV) technology. The average annual growth rate for solar PV is the highest at 37% and is expected to increase over the years [1]. Recently, crystalline Silicon (Si) based technology accounts for the largest market share in the photovoltaic industry due to higher efficiency compared with other commercially available technologies [2–4]. The Si-based modules have an average efficiency from about 10% to 15%, depending on the specific geographical location.

However, a main limitation with the present silicon-based module is the performance degradation caused by the strong dependency on solar irradiance and ambient temperature. The module temperature is determined by the equilibrium between electrical power generated and heat wasted in the PV module by the sun through conduction, convection, and radiation [5]. In principle, solar PV absorbs 80% of incident solar irradiance, but only 20% is transformed into electricity [6]. A significant portion of absorbed sunlight cannot be converted into electricity but wasted as heat, causing an unwanted increase in module temperature. The percentage of

* Corresponding author.

E-mail address: iadnan@ukm.edu.my (A. Ibrahim).

temperature degradation ranges from 0.25%/°C to 0.5%/°C and is defined as the temperature coefficient [7]. The conversion efficiency limitations caused by an unwanted temperature increment have led to research into cooling alternatives. By applying an efficient cooling technique, the PV lifetime can be prolonged for more than 30 years.

Numerous studies have been conducted on different PV cooling methodologies and can be divided into passive and active cooling. An active cooling method was found to perform better in terms of reducing the module temperatures. However, a detailed review [8–11] on cooling methodologies reported that passive cooling is more promising than active cooling. They require no auxiliary input power and are economically viable for a big-scale PV deployment.

In PV passive cooling method, there are three practical approaches, including the use of phase change materials (PCMs), aluminum fin heat sinks, and radiative cooling. As shown in Fig. 1(a)–(c), respectively, researchers have investigated the use of PCM to cool the PV [12–14]. Although their findings are promising, the use of PCM is limited by its high cost, low thermal conductivity, phase segregation, and fire safety. On the other hand, recent studies on radiative cooling [15–17] were conducted but reported achievable under suitable atmospheric conditions. Such a method would require further research and development since it involves modifying commercially available silicon solar cells. Recent studies relevant to the present work were investigated in papers [18–21] -please see Fig. 1(d)–(e) respectively. Those methods were based on Newton’s Law of cooling by increasing the heat transfer area through aluminum material attached to the backside of PV modules. This method can be considered the most economical compared to the other passive cooling techniques, technically feasible under different climatic conditions, and easily implemented, as they operate without consuming energy.

1.1. Research contribution

Conventionally, it is assumed that PV modules operate at a single temperature, but this is not the case. Instead, the modules experience varying environmental conditions causing the temperature non-uniformity distribution. Failure to improve the non-uniformity leads to a higher dissipation of power and breakdown in localised regions [22]. The effect of temperature non-uniformity across PV modules can cause a current imbalance between series-connected cells, leading to a reverse-biased phenomenon [23] that will degrade the modules’ performance. Although various work has been conducted in the research of passively PV cooling using fins, none of the studies has emphasised the PV module’s temperature non-uniformity behaviour. In addition, most past studies were tested on non-commercialised PV modules with smaller collector areas as in Refs. [24,25], and the temperature uniformity was not a concern. Therefore, a detailed study on the temperature uniformity of fin-cooled PV modules is not available in the literature.

This paper aims to investigate passive cooling of PV modules using a novel fins heat sinks design called multi-level fin heat sinks (MLFHS). Also, unlike previous researchers, to bridge the gap between lab-scale work and industrial applications, the passive cooling approach in this work was conducted on a commercial PV module, i.e. not at the lab-scale size. Temperature uniformity across the passively cooled PV module is being investigated under outdoor operating conditions.

To achieve the aims, the methodology of the research is categorised into three key stages. The first is to experimentally investigate

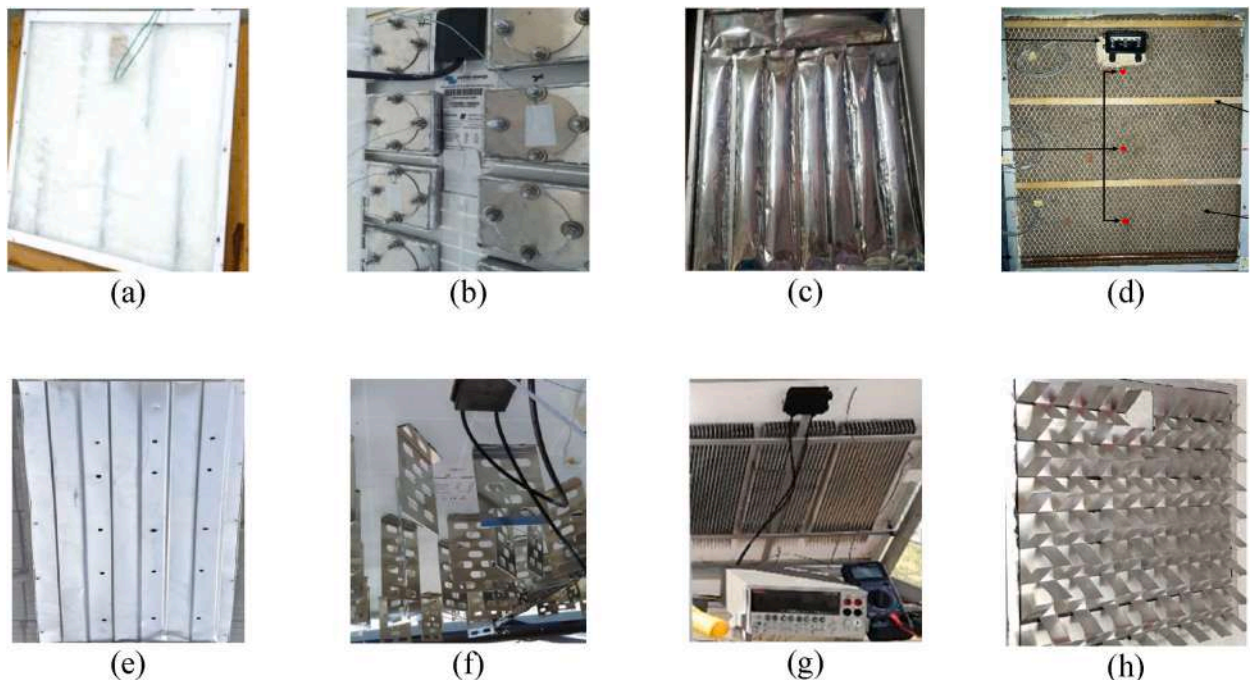


Fig. 1. Recent passive cooling methodologies: (a)–(c) using PCM as in Refs. [12–14] respectively, and (d)–(e) using aluminum fins heat sin as in [18–21].

the influences of the proposed novel heat sinks on the temperature uniformity across the PV module. Here, the proposed novel multi-level fin heat sinks design (MLFHS) concept is detailed and justified. The second is to examine the temperature non-uniformity across the PV panel. The effect of heat sinks on the temperature uniformity across collector areas under outdoor operating conditions was performed. Finally, we have investigated the influences of heat sinks on electrical output performance. These findings are foundational for future improvements in cooling methodologies, especially for passive cooling approaches.

2. Theoretical background

2.1. Temperature uniformity and electrical performances

The temperature uniformity on the surface of the PV module is an important parameter to be investigated to avoid the current mismatching problems. It is favourable to achieve a value of uniformity closer to 1. Hence, the temperature uniformity in this work is investigated and analysed using the following equation [27]:

$$\%T_{uni} = \left[1 - \frac{T_{max} - T_{min}}{T_{avg}} \right] \times 100\% \tag{1}$$

The operating temperature of a PV module plays a vital role in the energy conversion process.

Various methods have been proposed in the literature to determine the module operating temperature through simplified working equations [28–31]. However, the following equation is widely used to determine the module efficiency described as follows, which later will be discussed in section 4:

$$\eta = \eta_{STC} [1 - \beta(T_{pv} - T_{STC}) + \gamma \text{Log}G] \tag{2}$$

η_{STC} is the module efficiency at PV module temperature = T_{STC} (25 °C), G is the solar irradiance measured in W/m^2 , and T_{pv} is the PV module temperature. β and γ are the coefficients for the temperature and solar irradiance, respectively. The values for η_{STC} , β , and γ are given in the module datasheet. In most cases, Eq. (2) is seen with $\gamma = 0$ and can be expressed as follows:

$$\eta = \eta_{STC} [1 - \beta(T_{pv} - T_{STC})] \tag{3}$$

In a comparative study concerning power output performance, the percentage difference was performed using the following equation:

$$\%P_{out} = \frac{P_{out_fin} - P_{out_ref}}{P_{out_ref}} \times 100 \tag{4}$$

3. Materials and methods

3.1. Photovoltaic panels

The photovoltaic panels used in the experiment consist of the following:

- i. Monocrystalline PV modules of 120 Wp with the specifications presented in Table 1.
- ii. The truncated Multi-Level Fin heat sink (MLFHS) design is proposed to reduce the stagnation zone within the heat sinks by inducing more air turbulence, thus better heat transfer. The heat sinks were fabricated from a commercially available Aluminum alloy 6063, as illustrated in Fig. 2. The fin design parameters are shown in Table 2.

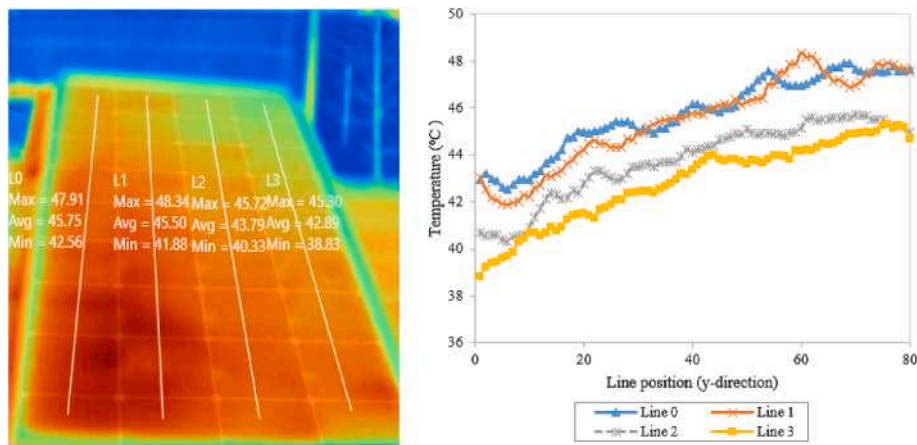


Fig. 2. The PV module (without fins) exhibits non-uniform temperature distributions.

- iii The Aluminum fins were attached using epoxy resin with metal powder (Devcon R2-42). The epoxy assists in eliminate air gaps while improving thermal conductivity.

3.2. The heat sink design

Previous studies have investigated various fin geometries to reduce the module temperature. However, the influence on temperature distributions across the PV module was not being considered because the proposed fins were based on a single temperature measurement. However, that is not the case. Under outdoor operating conditions, the module experience varying ambient conditions hence exhibits non-uniform temperature distributions. Thus, maintaining the temperature uniformity across the PV module is equally important as reducing the operating temperature [22,32]. Therefore, the novelty of the proposed fins aims to improve the temperature non-uniformity by flattened the PV temperature curves in Fig. 3 The experimental setup consists of the truncated multi-level fins heat sink (MLFHS) installed at the backside of the PV module. The MLFHS configuration consisted of dual fins height (40 and 60 mm) to induce air flows under natural convection. Besides, the fins were truncated (L-shaped) to exhibit a better heat dissipation rate per unit mass compared with the conventional heat sink. (see Fig. 3).

3.3. The experimental setup

The experimental setup was developed to evaluate the PV module performances under the local climate conditions of Malaysia (2.1896° N, 102.2501° E). The setup consists of two identical monocrystalline PV modules with dimensions of 1190 × 540 × 35 mm, inclined at 18 ° facing the south. One module was used as a reference, while the other with an attached MLFHS for cooling, as illustrated in Fig. 4. The monitoring and equipment measurements are based on the Malaysia Standard MS IEC 61724:2010: Photovoltaic system performance Monitoring-Guidelines for measurement, data exchange, and analysis. (see Table 3). The current-voltage measurement and the weather monitoring station were used for the electrical and thermal analysis, and the experimental setup is presented in Fig. 4.

3.4. PV module acceptance test and uncertainty analysis

The acceptance test is conducted at the test site to ensure the PV modules perform within manufacturer specifications and verify their functionality. The minimum requirement to conduct the acceptance test is to ensure the solar irradiance levels should be at least 350 W/m². In addition, the percentage difference between expected and measured values for V_{oc} and I_{sc} should be within ± 5 %. Both PV modules were tested, and the acceptance results are presented in Table 4.

The uncertainty analysis for the test instrumentations was determined based on the following equation [26]:

$$\Delta U = \pm \sqrt{\Delta U_{dc}^2 + \Delta U_{ms}^2} \quad (5)$$

The declared uncertainty (ΔU_{dc}) for temperature, current, and voltage are based on the equipment datasheet provided by the manufacturer, while measurement uncertainty (ΔU_{ms}) depends on the measurements taken under actual operating conditions.

4. Results and discussions

4.1. The effect of fin heat sinks on the PV module temperature

The measured solar irradiance and ambient temperature are presented in Fig. 5. Since Malaysia is located near the equator, the climate is categorised as equatorial, hot, humid, and cloudy throughout the year. The recorded temperatures were high and stable between 29 °C to 38 °C throughout the day, even when the solar irradiance dropped below 600 W/m². It should be noted that cloudy conditions have occurred in the morning from 9:00 to 13:00, causing the ambient temperature to drop below 34 °C. The highest and lowest solar irradiance values of 941 W/m² and 196 W/m² were recorded at 12:55 and 17:00, respectively.

Fig. 6 shows the temperature changes of the PV modules recorded from 9:00 to 17:00. The module temperatures with and without fin heat sinks were between 33.65 to 58.74 °C and 36.14 to 62.31 °C, respectively. This figure shows one peculiarity: fin heat sinks demonstrate a significant impact on module temperature reduction at high solar irradiance (>650 W/m²), which can be observed from



Fig. 3. The proposed truncated Multi-Level Fin Heat Sink (MLFHS).

Table 1
Details of examined PV module at standard testing conditions (STC).

Parameters	Value
Maximum power (STC) (P_{max})	120 Wp
Open-circuit voltage (V_{oc})	24.64 V
Short-circuit current (I_{sc})	6.21 A
Maximum operating voltage (V_{mp})	20.88 V
Maximum operating current (I_{mp})	5.75 A
Operating temperature	$-40\text{ }^{\circ}\text{C}$ to $+85\text{ }^{\circ}\text{C}$
Power temperature coefficient (γ)	$-0.35\%/^{\circ}\text{C}$
Voltage temperature coefficient (β)	$-0.27\%/^{\circ}\text{C}$
Current temperature coefficient (α)	$0.05\%/^{\circ}\text{C}$

Table 2
The proposed fins design parameters.

Geometric parameters	Value	Unit
Length of heat sinks (L)	800	mm
Width of heat sinks (W)	400	mm
Fin height (h)	40, 60	mm
Fin spacing (s)	20	mm
Fin thickness (t)	1.0	mm

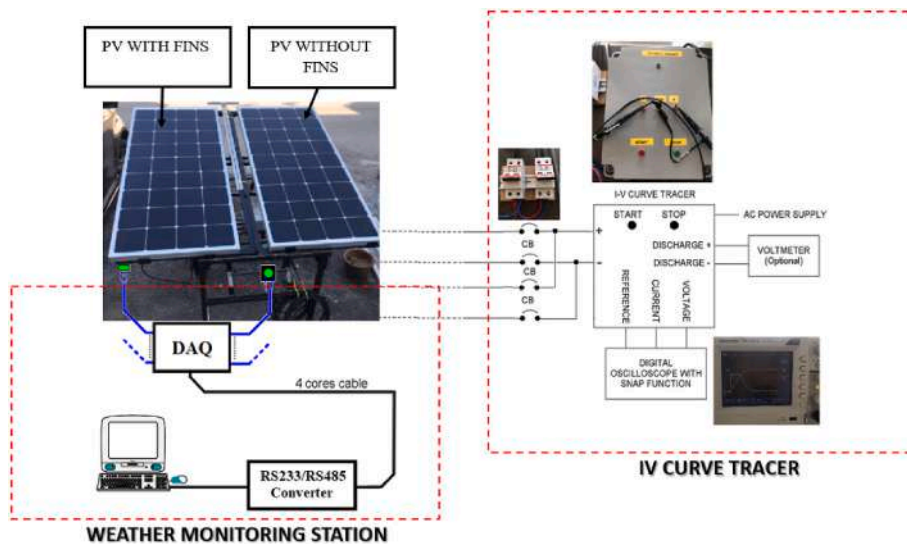


Fig. 4. The experimental setup.

noon onwards. On the other hand, the temperature reductions between panels were nearly consistent between 7.50 and 8.45 °C starting in the mid-afternoon even though the solar irradiance levels were toward the downtrend in the evening. These findings suggested that fin heat sinks utilisation positively influences the temperature reduction of PV modules, especially for PV modules near the equator, but less impact and not economical for countries with average solar irradiance below 500 W/m².

4.2. The effect of fin heat sinks on the temperature distribution across the PV module

The module temperature is significantly reduced with the utilisation of the fin heat sink. Although lowering the temperature can improve the module efficiency, maintaining the temperature homogeneity across the PV module can further enhance its efficiency and lifespan by reducing the hotspot phenomenon [33]. Hence, temperature uniformity has been considered for the fin heat sink design. Initially, an investigation was conducted on the inclined (15°) bare PV module to observe the temperature distribution. Regions across the tested module were classified as top, middle and bottom. During these measurements, the average irradiance and the ambient temperature levels were in the range of 858–882 W/m² and 26–38 °C, respectively. Based on Fig. 7, the recorded thermal images for the module exhibited inhomogeneity indicated by the reference line positions in the y-direction (L0, L1, L2, and L3). The middle and bottom regions have relatively higher temperatures than the top module by $\pm 6\text{ }^{\circ}\text{C}$. The top region exhibits lower temperature distributions due to the inclined PV module (18 ° facing the south). The top module is relatively higher from the ground, allowing for

Table 3
Data acquisition devices and their specifications.






Instruments	Image	Model	Specifications
Digital multimeter		SANWA DCM400AD	Uncertainty: 0.5% Accuracy: DCA: $\pm (2.5\% \pm 10)$ Resolution: DCA: 0.01 A
Thermal imager		FLUKE TIR125	Uncertainty: 0.08% Accuracy: $(\pm 2.0^\circ\text{C})$ Range: $-20^\circ\text{C} \sim +150^\circ\text{C}$
Irradiance meter		SEAWARD Solar survey 200R	Uncertainty: 0.5% Accuracy: $(\pm 1.0\%)$
Thermocouples		K-type (chromel-alumel) Fibreglass insulated	Uncertainty: 0.2% Accuracy: $(\pm 2.0^\circ\text{C})$ Range: $200^\circ\text{C} \sim 300^\circ\text{C}$
Anemometer		Anemometer Wind Sensor Gauges 4–20 mA	Uncertainty: 0.1% Accuracy: $(\pm 0.1\text{m/s})$

Table 4
The acceptance test for the examined PV modules.

Panel	Measured module temperature ($^\circ\text{C}$)	Irradiance (W/m^2)	Percentage difference (%)		Accept (A) or Reject (R)	
			V_{oc}	I_{sc}	V_{oc}	I_{sc}
A	42.8	545	1.52	1.73	A	A
B	43.1	551	1.43	1.68	A	A

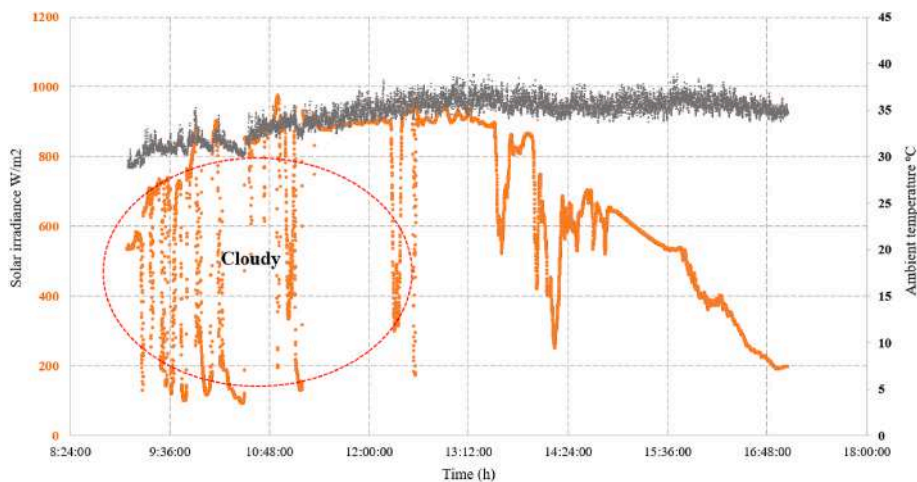


Fig. 5. Solar irradiance and ambient temperature distribution recorded at the test site.

better airflows than the middle and bottom regions.

To further investigate the effect of fin heat sinks, thermal mappings were performed on both PV modules. The module with the heat sink was exclusively compared with the reference PV module. Fig. 8(a–c) shows IR images for both modules, measured at 9:00 a.m., 12:00 p.m., and 3:00 p.m. Based on the recorded IR images, the temperature reduction varies differently across the top, middle, and bottom areas. The maximum temperature difference between reference module and module with MLFHS was recorded at 8.45 $^\circ\text{C}$. It can be seen that the influence of heat sinks was significant at solar noon compared to in the morning and evening by 4.17%, 1.92%, and 2.16%, respectively. These findings strongly suggest that implementing cooling heat sinks for temperature reduction is feasible in hot weather countries that receive more than 600 W/m^2 of solar irradiance. Based on the measured data, the temperature uniformity for

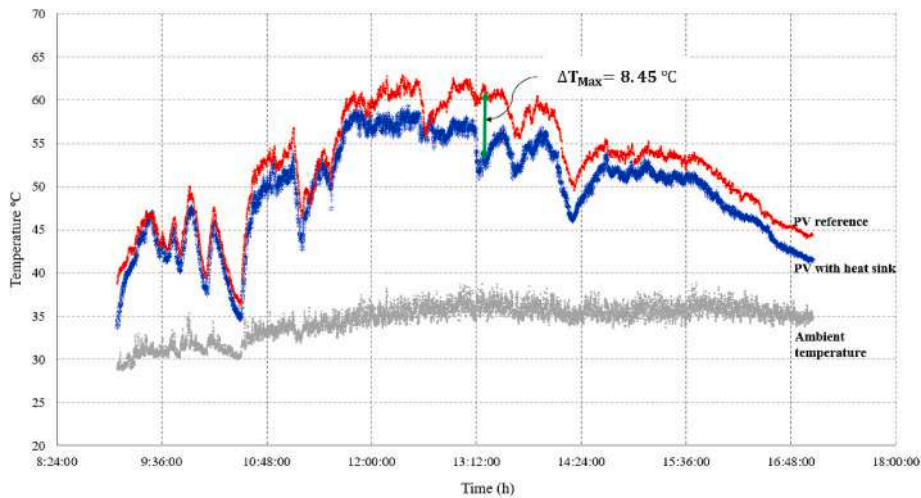


Fig. 6. Temperature variations between reference and finned PV module.

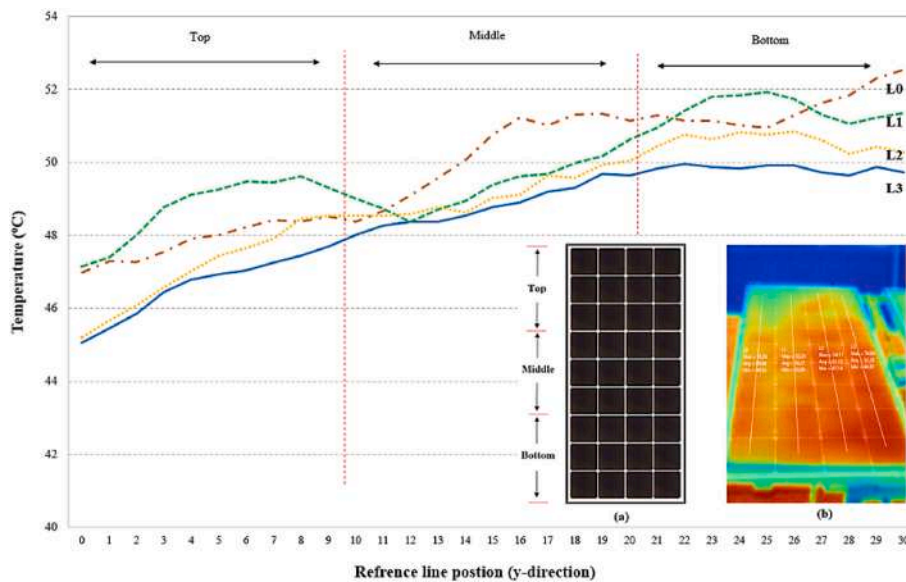


Fig. 7. Temperature variations across the PV module without cooling.

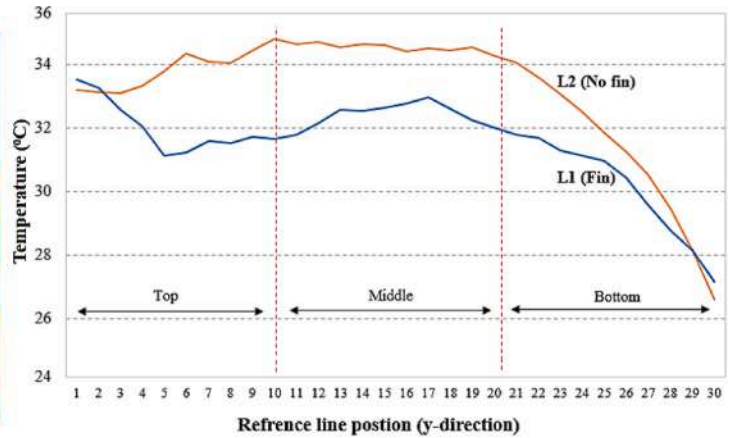
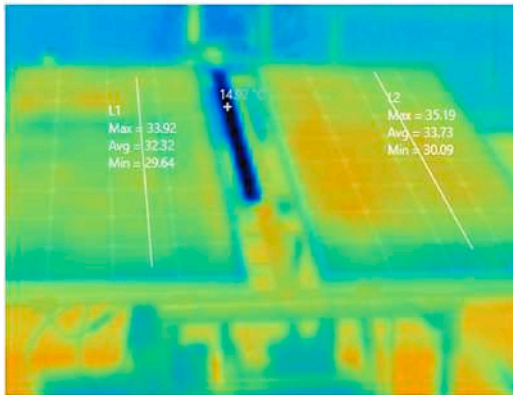
both modules was calculated using Equation (1). Table 5 shows the summarised results for the influence of fins on temperature uniformity. It was found that the average temperature uniformity was improved by at least 14.8% (see Table 6).

4.3. The influence of fin heat sink on the electrical performance parameters

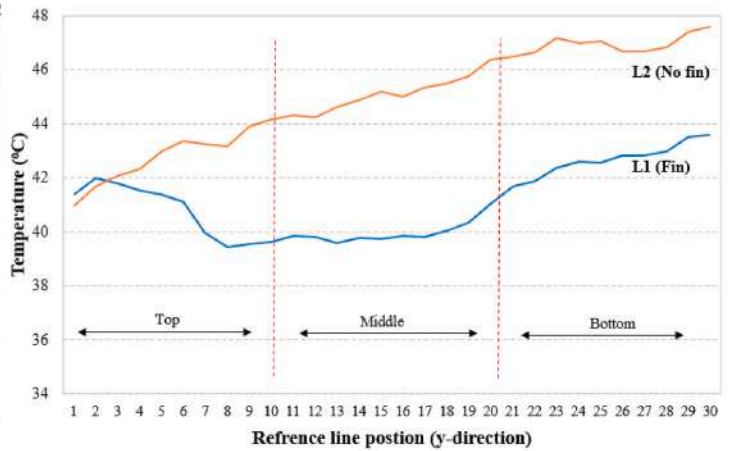
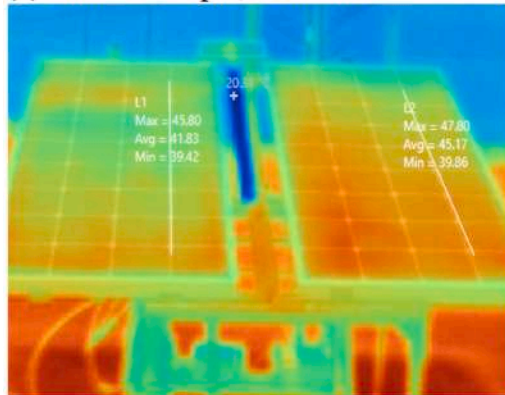
Temperature variations within the PV module can significantly impact the electrical output performance. Therefore, it is essential to characterise the PV module performance by a current-voltage curve. Several important electrical parameters, including short-circuit current (I_{sc}), open-circuit voltage (V_{oc}), current at maximum power (I_{mp}), and voltage at maximum power (V_{mp}) were measured and analysed. Fig. 9 shows the I–V curve for both PV modules tested under outdoor operating conditions. During these measurements, the average solar irradiance and the ambient temperature were in the range of 212–944 W/m² and 26–38 °C, respectively. The V_{oc} for the PV module with heat sink was observed to be higher than the reference module by at least 4.74%. Since solar cells are made up of semiconductor materials, increasing temperature increases excess electrons and holes, causing the greater depletion region width known as the charge separation layer. Hence, the V_{oc} is very much dependent on the temperature. The measured I_{sc} for the module with heat sinks was lower than the reference module, measured at 5.88 A and 6.10 A, respectively. The change of I_{sc} with temperature highly depends on the light trapping properties of the designed solar cell. Hence, it can be observed that the change in I_{sc} is much smaller than the V_{oc} (see Fig. 10).

As highlighted in the I–V curves, the square boxes represent the fill factor (FF) for both tested modules. The fill factor measures the

(a) Time: 9:00 am, Irradiance: 520 W/m²



(b) Time: 12:00 pm, Irradiance: 940 W/m²



(c) Time: 3:00 pm, Irradiance: 640 W/m²

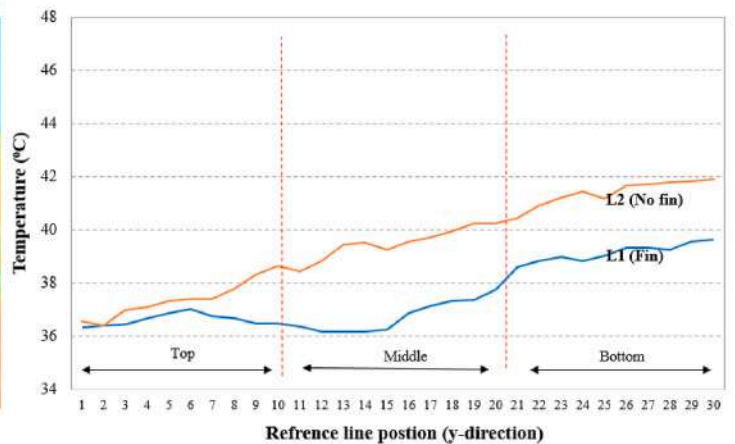
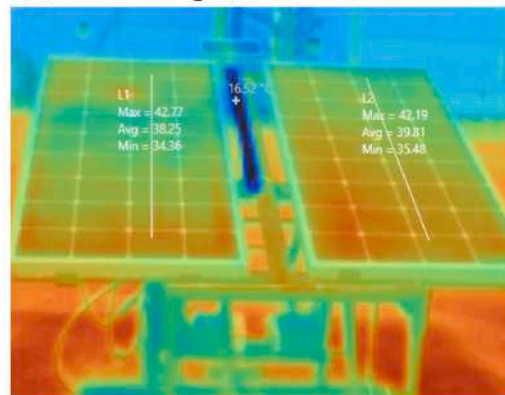


Fig. 8. The effect of aluminum fin heat sinks on the module operating temperature.

module efficiency, calculated by comparing the measured maximum power to the theoretical value calculated using Equation (3). The result shows that the fill factor for the reference PV module and PV module with heat sink are 0.57 and 0.63, respectively. The corresponding $P-V$ curves were determined based on the derived electrical parameters and presented in Fig. 10. The maximum output power (P_{max}) for PV reference and PV with heat sinks are 87.23 W and 96.61 W. However, the maximum power obtained from the PV with heat sinks (96.61W) is less than maximum power at standard testing conditions (120 W) because it is impossible to control the module temperature at 25 °C under outdoor operating conditions, especially in regions with high solar irradiance. The relative power is enhanced by 10.75%, higher than the reference PV module. The overall electrical performances for tested PV modules are

Table 5
Temperature uniformity.

Time	Irradiance, W/m ²	Temperature uniformity	
		PV (with fins)	PV (without fin)
9:00 a.m.	520	0.867	0.846
12:00 p.m.	940	0.847	0.820
3:00 p.m.	640	0.831	0.813

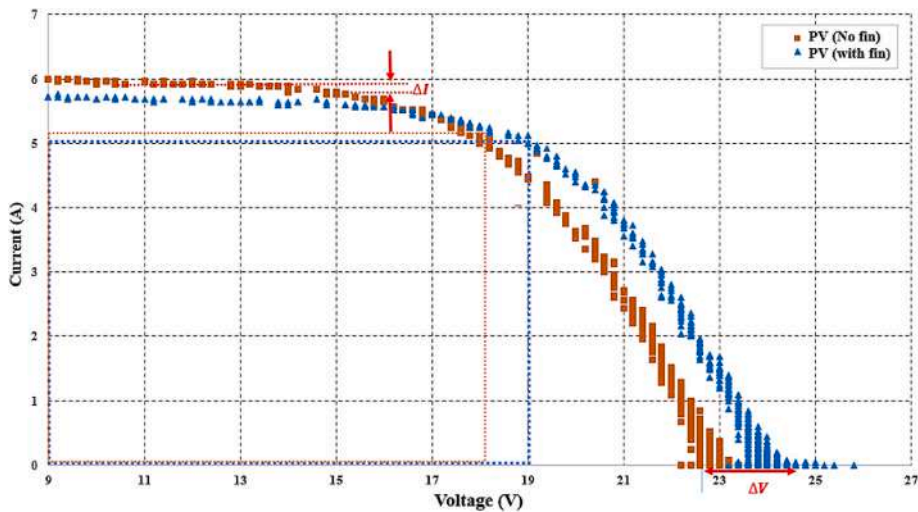


Fig. 9. Current-Voltage curves for the reference PV module and PV module with heat sinks at solar irradiance of 941 W/m², and ambient temperature of 36.17 °C.

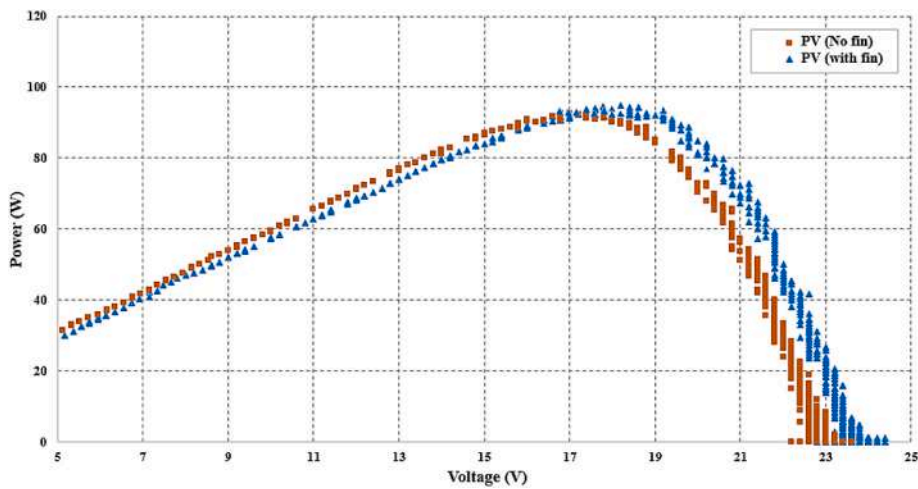


Fig. 10. Power-Voltage curves for the reference PV module and PV module with heat sinks at solar irradiance of 941 W/m², and ambient temperature of 36.17 °C.

summarised in Table 6. It is worth noting that when the module temperature drops, the voltage rises, resulting in a substantial increase in available maximum electrical power despite a slight decrease in short-circuit current.

5. Conclusions

This study investigated the effect of the proposed fin heat sink design as a passive cooling approach under outdoor operating conditions. The present study focuses on the fin heat sink design to achieve temperature uniformity across the PV module while improving the electrical output performances. Several important findings can be concluded in the following points:

Table 6
The overall electrical performances.

Electrical parameters	Measured data at an irradiance of 941 W/m ² and ambient temperature of 36.17 °C	
	PV (reference module)	PV + heat sink
Short-circuit current, I _{sc}	6.10 A	5.88 A
Open-circuit voltage, V _{oc}	22.4 V	23.8 V
Current at the maximum point, I _{mp}	4.64 A	4.98 A
Voltage at the maximum point, V _{mp}	18.8 V	19.4 V
Maximum power, P _{max}	87.23 W	96.61 W
Fill factor, FF	0.57	0.63

- The module operating temperature for PV reference and PV with proposed MLFHS are recorded at 64.2 °C and 56.1 °C, respectively. The proposed MLFHS exhibits better temperature reduction compared to conventional PV module by up to 8.45 °C.
- The maximum electrical power output increases up to 10.75% by integrating the proposed MLFHS at the backside of the PV module.
- The heat sink effect on the temperature uniformity was improved by at least 14.8%.
- The proposed new fin heat sink design is a viable solution and economical to achieve temperature uniformity as the hotspot phenomenon can lead to mechanical damage and reduce its lifespan.

Author statement

E. Z. Ahmad devised the conceptual ideas, including writing, reviewing, designing the model, computational framework, data analysis, and draft preparation. A. Fazlizan, H. Jarimi and K. Sopian verified the analytical methods and investigation. A. Ibrahim performed the visualization, funding acquisition and supervised the findings of this work.

Declaration of competing interest

The authors declare that they have no known competing financial interests or personal relationships that could have appeared to influence the work reported in this paper.

Acknowledgement

The authors would like to acknowledge the support for this research by Solar Energy Research Institute, Universiti Kebangsaan Malaysia (UKM) through research funding FRGS/1/2019/TK07/UKM/02/4 (Fundamental Research Grant Scheme).

References

- [1] International Energy Agency, Global Energy & CO₂ Status Report, 2018.
- [2] M.A. Green, Photovoltaic Technology and Visions for the Future, " *Prog. Energy*, 2019.
- [3] S. Nizetić, E. Giama, A.M. Papadopoulos, Comprehensive analysis and general economic-environmental evaluation of cooling techniques for photovoltaic panels, Part II: active cooling techniques, *Energy Convers. Manag.* 155 (July 2017) (2018) 301–323.
- [4] A. Ibrahim, S. Mat, A. Fudholi, A. F. Abdullah, and K. Sopian, "Outdoor performance evaluation of building integrated photovoltaic thermal (BIVPT) solar collector with spiral flow absorber configurations," *Int. J. Power Electron. Drive Syst.*, vol. 9, no. December, pp. 1918–1925, 2018, doi: 10.11591/ijpeds.v9n4.pp1918-1925.
- [5] J.A. Duffie, W.A. Beckman, *Solar Engineering of Thermal Processes*, fourth ed., 2013.
- [6] A.M. Elbreki, A.F. Muftah, K. Sopian, H. Jarimi, A. Fazlizan, A. Ibrahim, Experimental and economic analysis of passive cooling PV module using fins and planar reflector, *Case Stud. Therm. Eng.* 23 (November 2020) (2021) 100801.
- [7] O. Dupré, R. Vaillon, M.A. Green, *Thermal Behavior of Photovoltaic Devices*, 2017.
- [8] S. Nizetić, A.M. Papadopoulos, E. Giama, Comprehensive analysis and general economic-environmental evaluation of cooling techniques for photovoltaic panels, Part I: passive cooling techniques, *Energy Convers. Manag.* 149 (2017) 334–354.
- [9] E.Z. Ahmad, et al., Recent advances in passive cooling methods for photovoltaic performance enhancement, *Int. J. Electr. Comput. Eng.* 11 (1) (2021) 146–154, <https://doi.org/10.11591/ijece.v11i1.pp146-154>.
- [10] P. Dwivedi, K. Sudhakar, A. Soni, E. Solomin, I. Kirpichnikova, Advanced cooling techniques of P.V. modules: a state of art, *Case Stud. Therm. Eng.* 21 (Oct. 2020) 100674.
- [11] N. Mat Wajid, et al., Solar adsorption air conditioning system – recent advances and its potential for cooling an office building in tropical climate, *Case Stud. Therm. Eng.* 27 (May) (2021) 101275.
- [12] S.V. Chavan, D. Devaprakasam, Improving the performance of solar photovoltaic thermal system using phase change material, *Mater. Today Proc.* 46 (2021) 5036–5041.
- [13] S. Nizetić, M. Jurčević, D. Čoko, M. Arıcı, A novel and effective passive cooling strategy for photovoltaic panel, *Renew. Sustain. Energy Rev.* 145 (October 2020) (2021).
- [14] P. Sudhakar, R. Santosh, B. Asthalakshmi, G. Kumaresan, R. Velraj, Performance augmentation of solar photovoltaic panel through PCM integrated natural water circulation cooling technique, *Renew. Energy* 172 (2021) 1433–1448.
- [15] S. Lv, Y. Ji, Z. Qian, W. He, Z. Hu, M. Liu, A novel strategy of enhancing sky radiative cooling by solar photovoltaic-thermoelectric cooler, *Energy* 219 (2021) 119625.
- [16] M. Hu, et al., An analytical study of the nocturnal radiative cooling potential of typical photovoltaic/thermal module, *Appl. Energy* 277 (July) (2020) 115625.
- [17] D. Sato, N. Yamada, Review of photovoltaic module cooling methods and performance evaluation of the radiative cooling method, *Renew. Sustain. Energy Rev.* 104 (July 2018) (2019) 151–166.
- [18] E.B. Agyekum, S. PraveenKumar, N.T. Alwan, V.I. Velkin, S.E. Shcheklein, Effect of dual surface cooling of solar photovoltaic panel on the efficiency of the module: experimental investigation, *Heliyon* 7 (9) (2021) e07920.

- [19] F. Grubišić Čabo, S. Nizetić, E. Giama, A. Papadopoulos, Techno-economic and environmental evaluation of passive cooled photovoltaic systems in Mediterranean climate conditions, *Appl. Therm. Eng.* 169 (January) (2020).
- [20] F. Bayrak, H.F. Oztop, F. Selimefendigil, Experimental study for the application of different cooling techniques in photovoltaic (PV) panels, *Energy Convers. Manag.* 212 (February) (2020) 112789.
- [21] J.G. Hernandez-perez, J.G. Carrillo, A. Bassam, M. Flota-banuelos, L.D. Patino-lopez, Thermal performance of a discontinuous finned heatsink profile for PV passive cooling, *Appl. Therm. Eng.* 184 (October 2020) (2021) 116238.
- [22] A. Pavgi, J. Oh, J. Kuitche, S. Tatapudi, G. Tamizhmani, Thermal Uniformity Mapping of PV Modules and Plants, 2017, pp. 1877–1882.
- [23] M. Simon, E.L. Meyer, Detection and analysis of hotspot formation in solar cells, *Sol. Energy Mater. Sol. Cells* 94 (2) (2010) 106–113.
- [24] A.M. Elbreki, K. Sopian, A. Fazlizan, A. Ibrahim, Case Studies in Thermal Engineering an innovative technique of passive cooling PV module using lapping fins and planner reflector, *Case Stud. Therm. Eng.* 19 (January) (2020) 100607.
- [25] F. Grubišić-Čabo, S. Nizetić, D. Čoko, I. Marinić Kragić, A. Papadopoulos, Experimental investigation of the passive cooled free-standing photovoltaic panel with fixed aluminum fins on the backside surface, *J. Clean. Prod.* 176 (2018) 119–129.
- [26] M. Dida, S. Boughali, D. Bechki, H. Bouguettaia, Experimental investigation of a passive cooling system for photovoltaic modules efficiency improvement in hot and arid regions, *Energy Convers. Manag.* 243 (2021) 114328.
- [27] A.A.B. Baloch, H.M.S. Bahaidarah, P. Gandhidasan, F.A. Al-sulaiman, Experimental and numerical performance analysis of a converging channel heat exchanger for PV cooling, *Energy Convers. Manag.* 103 (2015) 14–27.
- [28] M. Mittal, B. Bora, S. Saxena, A.M. Gaur, Performance prediction of PV module using electrical equivalent model and artificial neural network, *Sol. Energy* 176 (October) (2018) 104–117.
- [29] A.M. Muzathik, Photovoltaic Modules Operating Temperature Estimation Using a Simple Correlation, vol. 4, 2014, pp. 151–158.
- [30] a) H. Zainuddin, S. Shaari, A.M. Omar, S.I. Sulaiman, Z. Mahmud, F. Muhamad Darus, Prediction of module operating temperatures for free-standing (FS) photovoltaic (PV) system in Malaysia, *Int. Rev. Model. Simulations* (2011);
b) H. Zainuddin, M.S. Sallo, S. Shaari, A.M. Omar, S.I. Sulaiman, Photovoltaic module temperature profile for Malaysia, in: 2015 IEEE Conf. Energy Conversion, CENCON 2015, 2015, pp. 469–473, <https://doi.org/10.1109/CENCON.2015.7409590>.
- [31] H. Zainuddin, M.S. Sallo, S. Shaari, A.M. Omar, S.I. Sulaiman, Photovoltaic Module Temperature Profile for Malaysia, in: 2015 IEEE Conf. Energy Conversion, CENCON 2015, 2015, pp. 469–473.
- [32] M. Muneeshwaran, U. Sajjad, T. Ahmed, M. Amer, H. M. Ali, and C. C. Wang, "Performance improvement of photovoltaic modules via temperature homogeneity improvement," *Energy*, vol. 203, 2020.
- [33] E.L. Meyer, E.E. Van Dyk, The effect of reduced shunt resistance and shading on photovoltaic module performance, *Conf. Rec. IEEE Photovolt. Spec. Conf.* (2005) 1331–1334.